Individual alpha power predicts language comprehension

P. Wang[1], Y. He[3], B. Maess[1], J. Yue[5], L. Chen[2,6], J. Brauer[2,4], A.D. Friederici[2], T.R. Knösche[1*]

[1] Max Planck Institute for Human Cognitive and Brain Sciences, Brain Networks Group, Leipzig, Germany

[2] Max Planck Institute for Human Cognitive and Brain Sciences, Department of Neuropsychology, Leipzig, Germany

[3] Philipps University Marburg, Department of Psychiatry and Psychotherapy, Marburg, Germany

[4] Friedrich Schiller University, Office of the Vice-President for Young Researchers, Jena, Germany

[5] Harbin Institute of Technology, Laboratory for Cognitive and Social Neuroscience, School of Management, Harbin, China

[6] Beijing Normal University, College of Chinese Language and Culture, Beijing, China

Highlights

- Comprehension of structurally complexed embedded sentences is correlated with individual alpha power attenuation during task but not with alpha power at rest.
- These effects were localized in temporal-parietal brain regions known to be associated with language processing.

Data availability statement

Anonymized raw data will be made available upon request via email to the corresponding author provided the requesting researchers sign a formal data sharing agreement and cite this paper as origin of the data.

Corresponding author:

Thomas R. Knösche (knoesche@cbs.mpg.de)

Abstract

Alpha power attenuation during cognitive task performing has been suggested to reflect a process of release of inhibition, increase of excitability, and thereby benefit the improvement of performance. Here, we hypothesized that changes in individual alpha power during the execution of a complex language comprehension task may correlate with the individual performance in that task. We tested this using magnetoencephalography (MEG) recorded during comprehension of German sentences of different syntactic complexity.

Results showed that neither the frequency nor the power of the spontaneous oscillatory activity at rest were associated with the individual performance. However, during the execution of a sentences processing task, the individual alpha power attenuation did correlate with individual language comprehension performance. Source reconstruction localized effects in temporal-parietal regions of both hemispheres. While the effect of increased task difficulty is localized in the right hemisphere, the difference in power attenuation between tasks of different complexity exhibiting a correlation with performance was localized in left temporal-parietal brain regions known to be associated with language processing.

From our results, we conclude that in-task attenuation of individual alpha power is related to the essential mechanisms of the underlying cognitive processes, rather than merely to general phenomena like attention or vigilance.

1. Introduction

The alpha band (8-12 Hz) typically forms the most stable and prominent peak in the EEG/MEG power spectrum (Berger, 1938; Schomer & Da Silva, 2012). These oscillations evidently play a major role in brain function at rest, as their power is attenuated in the task-relevant brain regions during various movement or cognitive tasks, including finger tapping, driving, arithmetic calculations, and sentence comprehension (Gastaldon et al., 2020; Klimesch et al., 1990; Magosso et al., 2019; Mann et al., 1996; Pfurtscheller, 1989; Wang et al., 2021). The power attenuation in the alpha band has also been shown to scale with task demand or engagement at the group level (Magosso et al., 2019; Wang et al., 2021). This phenomenon has been associated with cortical activation or release from inhibition due to the task (Klimesch, 2012; Pfurtscheller, 2003). It has also been shown, at the individual level, that the alpha power at rest or immediately before the task correlates with task performance (Jones et al., 2010; Van Dijk et al., 2008; van Ede et al., 2012), but evidence for such an individual relationship for the task-related power attenuation during task performance is scarce (Hilla et al., 2020). Therefore, the question remains whether the attenuation phenomenon is related to the essential mechanisms of the underlying cognitive processes, rather than merely to general phenomena like attention or vigilance.

Moreover, the characteristics of the alpha peak (e.g., frequency and power) are specific for each individual (Furman et al., 2018; Grabot & Kayser, 2020; Gulbinaite et al., 2017; Horschig et al., 2014; Katyal et al., 2019; Migliorati et al., 2020; Minami et al., 2020; Sadaghiani & Kleinschmidt, 2016; Smit et al., 2006). Hence, the somewhat non-univocal picture on the relationship between individual alpha power dynamics and task performance might also be rooted in the insufficient capture of the individual oscillations by using the classical broad frequency band (about 8-12 Hz).

In order to clarify the question if the individual alpha power attenuation is related to cognitive performance, we turn to the arguably most 'human-like' cognitive faculty, namely language. The ability to produce and understand language requires intense coordination of numerous cognition faculties, such as phonological perception, syntax processing, semantic association, working memory, attention, and motor control. Indeed, it has been shown that the individual alpha peak frequency as well as

the alpha band power at rest are related to individual language abilities (Kwok et al., 2019; Rathee et al., 2020; Sklar et al., 1972). Recently, we have explored the alpha band power directly *during* a language task, and found an association between the alpha power attenuation and language task complexity (Wang et al., 2021). Consequently, we hypothesize that the difference in alpha power attenuation between language tasks of different complexity, gauged at the individual alpha peak frequency and in task-relevant brain regions, reflects the individual cognitive ability to handle the task, and hence might be associated with the observed performance.

In the present paper, we tested this hypothesis using the same data set as in our previously reported MEG study with healthy, native German adult speakers (Wang et al., 2021). On four days within a week, participants listened to complex German sentences, and answered probing questions regarding the thematic role assignment ("who is doing what to whom"). The sentences differed in their complexity by containing either single or double embedded relative clauses. Previously, we reported that the cortical (posterior superior temporal and adjacent parietal) alpha band power attenuation at the final embedding closure was significantly larger for double than for single embedded sentences (Wang et al., 2021). Here, rather than looking at the entire alpha band, we focus on the individual peak frequency obtained from the resting state. In particular, we examined the correlation between language performance and: (1) the individual peak frequency and its power at rest; (2) the power attenuation of the individual peak frequency during the experimental task at different syntactic positions in the sentences; (3) the spatial localization on the cortex for the observed correlation effects. The results confirm our hypothesis that the individual difference between the power attenuation for tasks of different complexities (double vs. single embedding sentence comprehension) correlates with the individual performance.

2. Materials and Methods

As we are reusing the data from our previous study, many of the methodological details are already described elsewhere (Wang et al., 2021). In the following, these aspects are just presented as brief summary.

2.1. Participants

Thirty right-handed native German speakers (fifteen females) were enrolled in this study (mean age: 27, range from 20 to 34). Their reading span was 3.7 ± 0.9 (mean $\pm$ SD). No neurological diseases or hearing impairments were reported. Participants were naïve to the purposes of the experiment and gave written informed consent prior to the experiment. The study was approved by the ethics committee of the University of Leipzig (number of this approval).

2.2. Stimulus material

Two types of German sentences with single and double hierarchical center embedding were presented (see Fig. S5). All sentences started with an introductory phrase followed by a relative clause initiated by a relative pronoun (e.g. dass / that). The beginning of each relative clause (brace) was labeled with *bxon* while the final verb of it was labeled with *bxoff* to indentify the same level of embedding. The place holder x represents the embedding level.

2.3. Experimental procedures

The experiment included four sessions carried out on four working days within one week. The stimuli were presented by the software 'Presentation' (www.neurobs.com). At each day, participants listened to 33 sentences of each sentence type (i.e. single and double embedded). Each participant received an individual randomization of all 264 sentences presented on the four days. None of the sentences was presented twice to the same participant. After each sentence, a content question was asked to test the understanding of the thematic role assignments. Each session comprised four blocks. Sentences were presented during the first three blocks. During the fourth block, resting-state was recorded for at least 10 minutes. Participants were asked to close their eyes and stay awake.

2.4. Behavioral data analysis

Behavioral performance was measured through the accuracy of the participants' responses to the question task. In contrast to our previous study, the single valued total performance accuracy of each participant was estimated by a simple mean across the 4 experimental days.

2.5. MEG data acquisition and preprocessing

After preprocessing, the data of the first three blocks (task sections) were epoched of 0.5 s length starting with the event triggers at *b1on, b1off, b2on, b2off, b3on, and b3off* (on for embedding's begin, and off for embedding's closure). Data of the fourth block (rest section, total 12min) were epoched into 36 trails of 20s length each to get a frequency resolution of 0.05 Hz for the determination of the peak frequency. After artifact rejection, the median value of number of valid trials was 34, ranging from a minimum of 6 to a maximum of 35.

2.6. Estimation of individual spontaneous peak frequency in sensor space

The individual spontaneous peak frequencies were estimated from the pre-processed resting-state MEG recordings. For each subject on each day, the power spectrum density (PSD) for each sensor was estimated using the multi-taper method via the function *psd_multitaper* from the MNE-python v.0.16 (Gramfort et al., 2013) (using default setup, except normalization = 'full'). The PSDs for each 20s-length trial were transformed to logarithmic scale (i.e., in dB) and then averaged cross trials and sensors. After the averaging, the 1/f pink noise background was estimated and subtracted from each average grand PSD. The maximal peaks between 7-29 Hz were identified as the individual peak frequency.

2.7. Estimation of individual peak frequency power during the task in source space

For source localization, we used individual single shell volume conductor models and source models constructed from the individual T1-weighted MR data. We utilized Freesurfer 6.0.0 to segment the inner skull as well as the cortical surface. Finally, the cortical surfaces were labeled according to Glasser et al. (2016). In this paper, we focused on the regions of interest (ROI), which showed significant alpha power difference for different sentence type at final closure of the embeddings (*b1off*), see Fig. 3A and Wang et al. (2021).

To estimate the alpha power in source space, we used the LCMV beamformer method (Van Veen et al., 1997) via the function *make_lcmv* by MNE-python v.0.16. The reconstructed current density was restricted to being perpendicular to the cortical

surface. The noise covariance matrix was computed by the mean noise covariance from the empty room measurements obtained before and after each recording session. A data covariance matrix was computed separately for each day based on the whole sentence data. The PSD (in dB) of each source was estimated using the multi-taper method (*psd_multitaper*, data zero-padding to 2 s), separately for each subject, ROI, sentence type, and day as mean over all presented sentences. The 1/f pink noise background was estimated and subtracted from each average PSD separately. To estimate the spectral power of the individual peak frequency at task, we averaged the spectral power of the two frequency bins, which define the interval around the individual peak frequency at rest. Finally, relative power attenuation was calculated by normalizing to the respective *b1on* power value separately for each subject, ROI, sentence type, and day. Hence, all subsequently reported spectral power values in task conditions are relative power attenuations with respect to *b1on*.

For computing the individual frequency power in Yeo's 17-networks (Yeo et al., 2011; Fig. 5A), we first morphed the individual source space to the fsaverage space via the source morph function in MNE-python v.0.16 (by setting fsaverage spacing „ico5"). The remaining steps were as same as for using the Glasser's ROIs.

3. Results

3.1. The individual resting-state peak frequency is not correlated with the language performance

We first examined the relationship between the individual peak frequency during rest (averaged across four days) and the total performance accuracy. The individual peak frequency was estimated from the resting-state recordings at sensor level (for more details, see Materials and Methods section 2.6.). We first estimated it for each subject on each day (Fig. 1A) and then averaged it across the four days (Fig. 1C). The overall task performance was calculated for each subject by averaging the accuracy scores of the four experimental days, including, both, double and single embedded sentences. As expected, for most participants, their individual peak frequencies were located in the alpha frequency range (8-12 Hz; Fig. 1A,C). There were 6 participants, though, whose peak frequencies were estimated in the beta range (> 16 Hz). We found no statistical difference among the estimated individual peak

210   frequencies of the four experimental days (Friedman's test Q = 0.71, p = 0.87; Fig.

211   1B). We also found no clear association between the 4-day-average individual peak

212   frequency and the total performance accuracy (Spearman's correlation, r = 0.20, p =
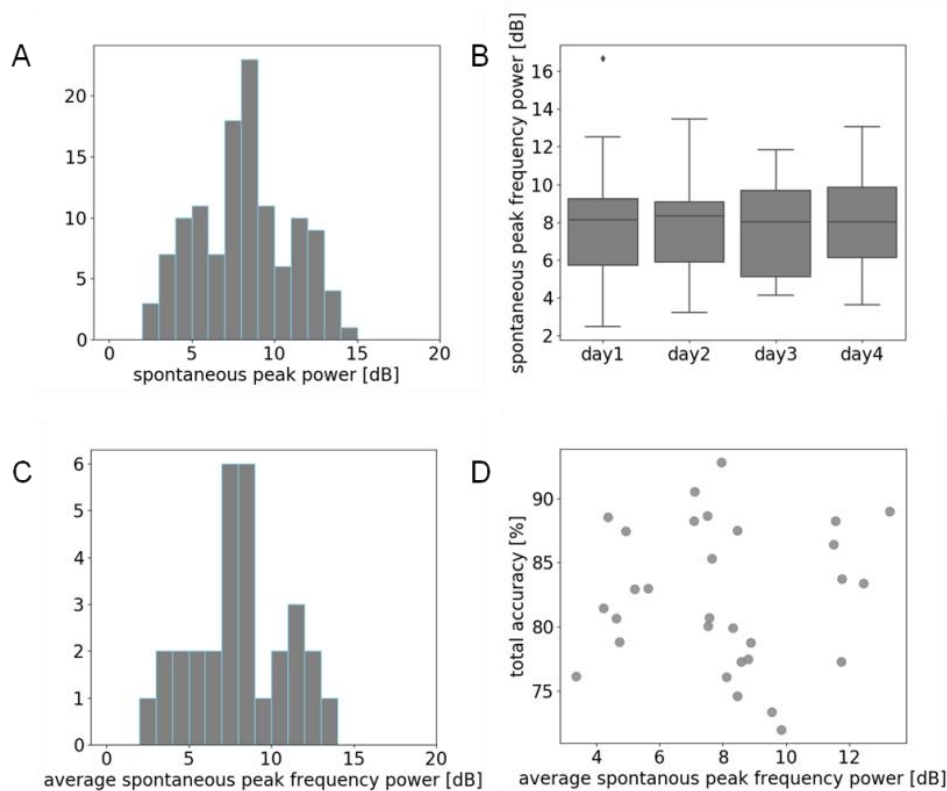
213   0.29; Fig. 1D).
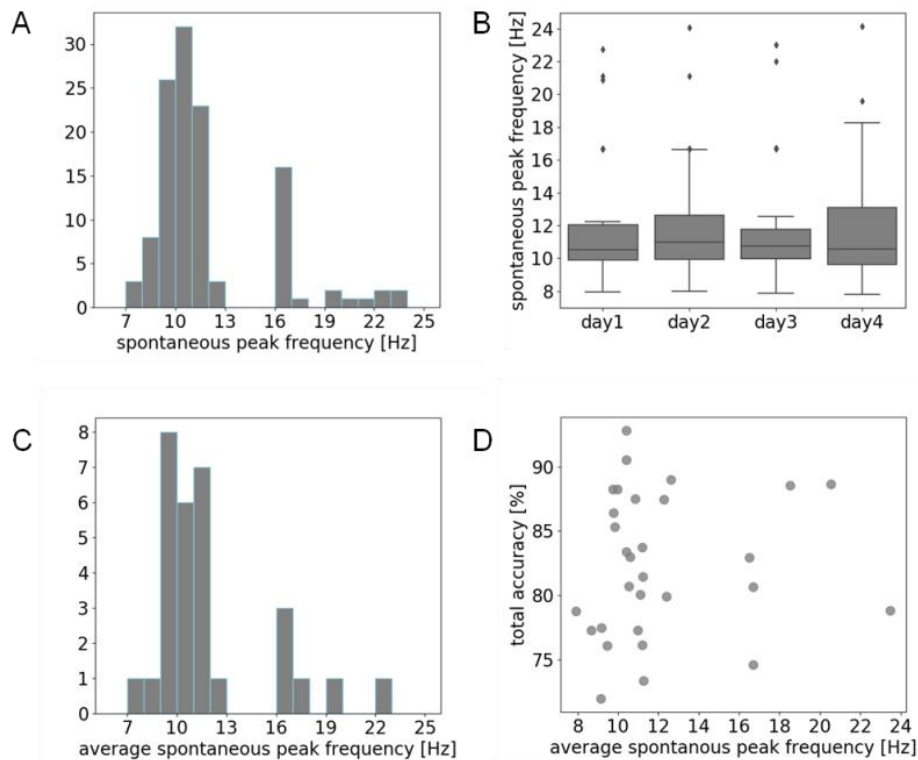
214

215   Figure 1. Relationship between the individual spontaneous peak frequency and the

216   language task performance. (A) Histogram of the 120 spontaneous peak frequencies

217   of the thirty participants on all four experimental days. (B) Boxplot of the participants'

218   individual spontaneous peak frequencies on each training day. The boxes show the

219   interquartile ranges that stretch from the first quartile (25th percentile) to the third

220   quartile (75th percentile) with the black line marking the median (50th percentile). The

221   maximal whisker range is 1.5 times the interquartile range. Note that the displayed

222   whisker length depends on values within whisker range. Diamonds represent outliers,

223   that is, values outside the whisker range. (C) Histogram of the thirty average

224   spontaneous peak frequencies per person, averaged over the four experimental days.

225   (D) Scatter plot showing the correlation between the total performance accuracy and

226   the spontaneous peak frequency, both averaged over experimental days.

227 *3.2. The power at the individual resting-state peak frequency is not associated with*
228 *the language performance*

229   Second, we examined the relationship between the power at the individual
230 peak frequency during rest (average across four days) and the total performance
231 accuracy. The power was also first estimated for each subject on each day (Fig. 2A)
232 and then averaged across the four days (Fig. 2C). There were no detectable power
233 differences between the four experimental days (Friedman's test Q = 3.0, p = 0.39;
234 Fig. 2B). We found no clear association between the (average) power and the
235 performance accuracy (Spearman's correlation, r = -0.09, p = 0.64; Fig. 2D).
236

239 Figure 2. Relationship between the power of individual spontaneous peak frequency
240 during rest and language task performance. (A) Histogram of the spontaneous peak
241 frequency power of the thirty participants for all four experimental days (120 values).
242 (B) Boxplot of participants' individual spontaneous peak frequency power for each
243 training day (for details, refer to Fig. 1). (C) Histogram of the spontaneous peak
244 frequency power of the thirty participants, averaged over the four experimental days.
245 (D) Scatter plot showing the correlation over participants between the total

246   performance accuracy and the average spontaneous peak frequency power. Total
247   performance accuracy was calculated by averaging the accuracy scores of the four
248   experimental days, including, both, double and single embedded sentences. Average
249   spontaneous peak frequency powers were averaged over experimental days (shown in
250   C).

251   *3.3. The power at the individual resting-state peak frequency during task was*
252   *associated with the language performance*

253   After examining the individual peak frequency and its power at rest, we
254   examined the power at the same individual frequencies when participants were
255   hearing the sentences, and tested its relationship with the language task performance
256   at single subject level. We expected that the *difference* in power attenuation between
257   the double embedded and single embedded sentences would reflect the subjects'
258   ability to process the sentences. To test this hypothesis, we focused on the brain
259   regions (Fig. 3A), for which in our previous study (Wang et al., 2021) we found a
260   significant difference in the alpha power (8-12 Hz) attenuation between the double
261   and single embedding conditions at the final closure of the embedding structure (*b1off*;
262   Fig. S5; for the meaning of the trigger point labels *b1on*, *b1off*, *b2on*, *b2off*, see
263   Materials and Methods section 2.2.). We first examined, whether by using the
264   individual resting-state peak frequency, we can replicate our previous result obtained
265   with the broad alpha band (sentence effect: general power attenuation difference
266   between double and singled embedded sentences). In Fig. 3B we show the power
267   decrease at the individual peak frequency at *b1off* (*b1off-b1on*) for each sentence type
268   and each day. A non-parametric ANOVA (Wobbrock et al., 2011) for the factors
269   sentence (double vs. single) and day (1 through 4) revealed only a significant main
270   effect for the factor sentence (F = 26.10, p = 7.44E-7). Averaged across all four days,
271   for both types of sentences, the alpha power decreases when sentence unfolds. The
272   difference between the power attenuation between sentence types increased over the
273   sentence and was most pronounced at *b1off* (Fig. 3C). The power attenuations at *b1off*
274   for single and double embedded sentences were strongly correlated (Spearman's
275   correlation r = 0.84, p = 9.00E-9; Fig. 3D).

276   Most importantly, as hypothesized, at *b1off*, the alpha power attenuation
277   difference between single and double embedded sentences was correlated with the
278   individual task performance (Spearman's correlation r = -0.64, p = 2.63E-5; Fig. 3E):

279   participants who showed a larger power attenuation difference between the two

280   sentence types at their individual peak frequency achieved better overall accuracy.

281   Moreover, those participants, who showed a larger power attenuation for the double

282   embedded sentences also performed better (Spearman's r = -0.44, p = 0.015; see

283   supplementary Fig. S1).

284   When using the classical frequency band (8-12 Hz, as reported in (Wang et al.,

285   2021) instead of the individual peak frequency, the by-subject correlation between

286   *b1off* power attenuation difference (double vs. single) and the performance reduced to

287   r = -0.50 (Spearman's correlation, p = 0.0049), and the correlation between the *b1off*

288   power attenuation for double embedding and the performance dropped to r = -0.28

289   (Spearman's correlation, p = 0.13; see supplementary Fig. S2).



290
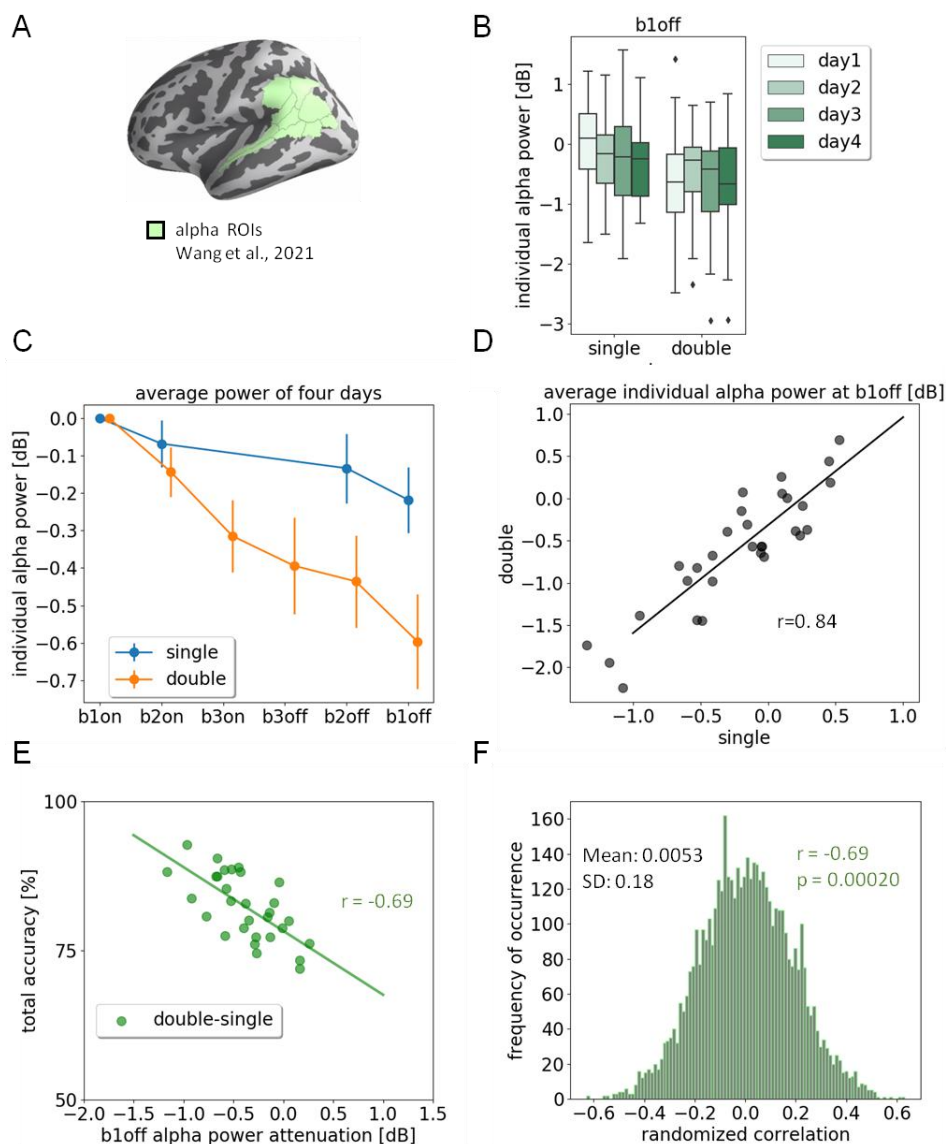
Figure 3. Relationship between the power attenuation at individual peak frequency during task and the language task performance. (A) Pre-selected ROIs that were reported to show significant power attenuation difference between double- and single embeddings at the final closure of the embedded structure in Wang et al., 2021. (B) Boxplot of the individual alpha power attenuation for each sentence type and each day. The individual alpha power attenuation was estimated by the power of the individual peak frequency at the final closure of the embedded structure (*b1off*) minus the power at the start of the embedded structure (*b1on*). (C) Four-days-average individual alpha power attenuation for each sentence type at different openings and closures of the embedded structure. Points show the mean value of the thirty participants, vertical lines show the standard error. The power of b1on (opening of the embeddings) was used as baseline for the other positions. (D) The individual alpha power attenuations at the final closures (*b1off*) for double and single embedded sentences were strongly associated (Spearman's correlation, p = 9.00E-9). (E) The power attenuation differences between double and single embedded sentences at the individual alpha frequency at the final closure were associated with the individual performance accuracy (Spearman's correlation, p = 2.63E-5). (F) Permutation-test of the association between the individual alpha power attenuation differences (double vs. single embedded sentence) at the final closure and the individual task performance. The power attenuations of the single as well as the double embedded sentences were permuted 5000 times. The mean of the randomized Spearman's correlation was 0.0053 and the standard deviation was 0.18. The probability of appearance of a correlation value that less than r = -0.69 was 0.0002.

3.4. Temporal exploration: association of alpha power attenuation and language performance at different embedding levels

Fig. 4A shows the Spearman's correlation between the total performance accuracy and the individual peak frequency power attenuation (i.e., with respect to *b1on*) for both sentence types at different positions of the embedded structure. Fig. 4B shows, at individual peak frequency, the power attenuation *difference* between the two sentence types at equivalent positions: *innerOn/innerOff* and *outerOn/outerOff* (opening/closure of the innermost/outermost embedded structures). After FDR-correction, we found three significant correlations. In addition to the power

324   attenuation at the final embedding closure for double embedded sentence and the

325   power attenuation difference at the final embedding closure, which were already

326   reported (Fig. 3E, & Fig. S1A), we found a performance correlation with the power

327   attenuation difference at the first embedding closure (*innerOff*; Spearman's r = -0.50 ,

328   FDR p<0.05; Fig. 4B).

∗ *FDR corrected p<0.05*
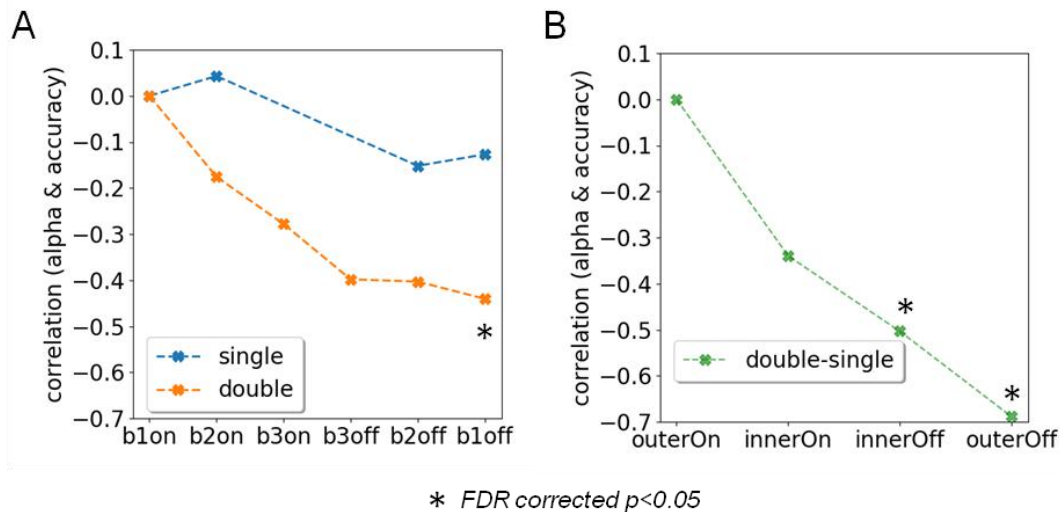
329

330   Figure 4. Association of the individual peak frequency power attenuation and the

331   language performance at different positions of embedded structures. (A)

332   Spearmans' correlation between the individual peak frequency power attenuation

333   (with respect to baseline b1on) for double and single embedded sentences and the

334   total performance accuracy. (B) Spearmans's correlation between the individual peak

335   frequency power attenuation difference (double-single) and the total performance

336   accuracy at different syntactically equivalent position. Position labels: outerOn: b1on

337   for single and double; innerOn: b2on for single and b3on for double; innerOff: b2off

338   for single and b3off for double; outerOff: b1off for single and double.

339

340   *3.5. Spatial exploration: association of individual peak frequency power attenuation*

341   *and language performance at the functional network level*

342   We explored the correlation between the individual peak frequency power

343   attenuation and the power attenuation difference (double vs. single embedding) of the

344   individual peak frequency at *b1off* and the total performance at the cortical level. In

345   order to achieve maximum specificity to functional networks, we used the Yeo's 17-

346   networks (Thomas Yeo et al., 2011) to define the brain ROIs (Fig. 5A). The power

347 attenuation difference in the left temporal-parietal network (including the anterior and
348 posterior superior temporal gyrus, Fig. 5A bright blue ROI) was significantly
349 correlated with task performance (Spearman's r = -0.62, FDR corrected p<0.05; Fig.
350 5B&C). Also, the power attenuation for double embedded sentence in the right
351 temporal-parietal network (including anterior and posterior superior temporal gyrus,
352 Fig. 5A bright blue ROI) was significantly correlated with the performance
353 (Spearman's r = -0.62, FDR corrected p<0.05; Fig. S3B&C).

354   Additional information about the spatial exploration of the correlation between
355 the individual peak frequency power attenuation at the final closure of the embedded
356 structure and the language performance based on the Glasser atlas (Glasser et al.,
357 2016) can be found in Fig. S5. We obtained similar results as for the Yeo's 17-
358 networks: in the left anterior and posterior superior temporal gyri, the power
359 attenuation difference between double and single embedded sentences was correlated
360 with the language performance, while in the right middle and posterior superior
361 temporal gyri, as well as inferior frontal gyrus, the power attenuation for double
362 embedded sentences was correlated with the performance.

363

364
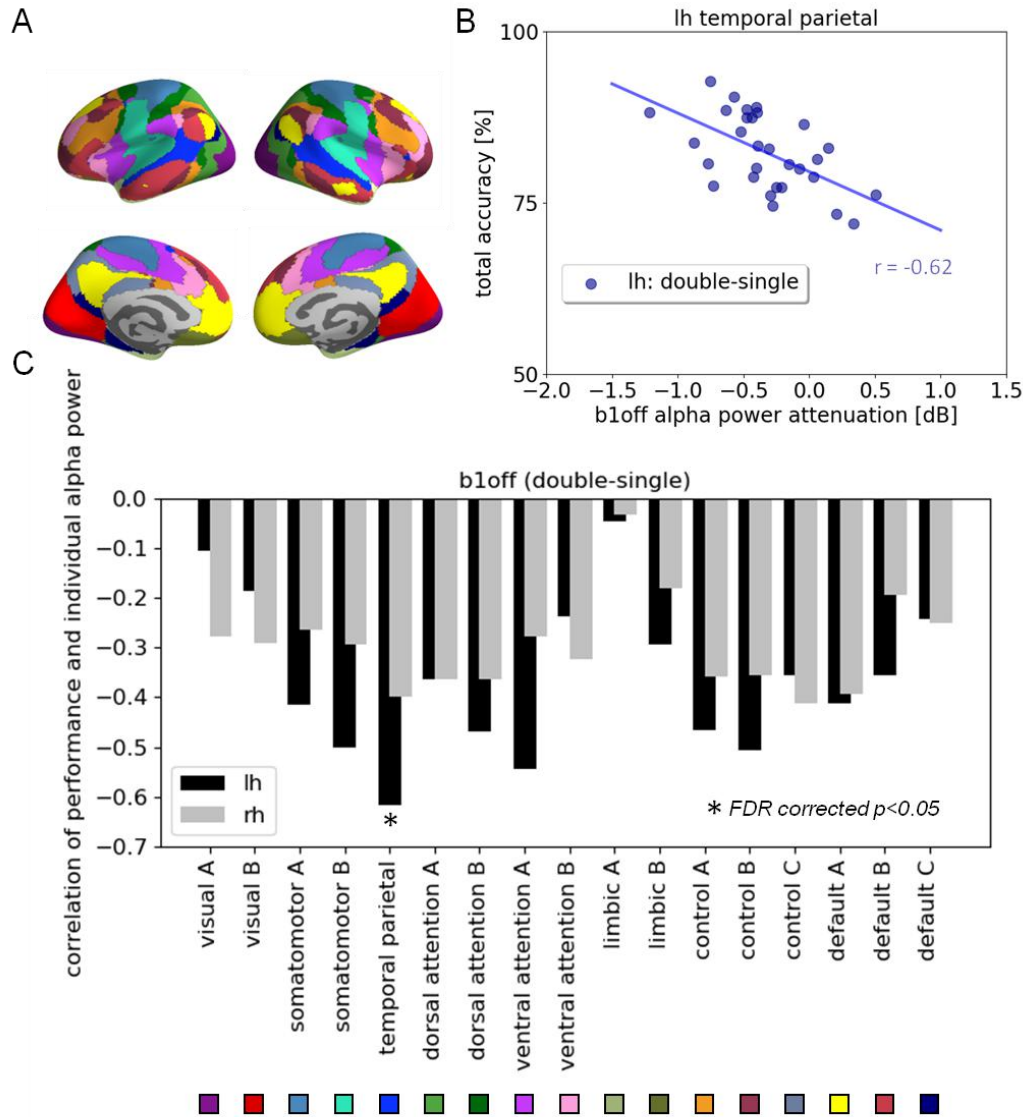
Figure 5. Association of the individual peak frequency power attenuation and the language performance at the functional networks level. (A) ROIs of Yeo's 17-networks. The temporal parietal network is painted in bright blue. (B) Individual peak frequency power attenuation difference (double vs. single embeddings) at the final closure of the embedded structures (b1off) in the left temporal-parietal network (lh: double-single) was significantly associated with the performance (Spearmans' r = -0.62, FDR corrected p<0.05). (C) Spatial distribution of the Spearman's correlation between individual peak frequency power attenuation difference (double vs. single embeddings) at the final closure of the embedded structures (*b1off*) and the individual performance accuracy on Yeo's 17-networks.

375

4. Discussion

In this study, we investigated the association between language comprehension performance and individual dominant oscillations under resting-state and in-task conditions. The individual peak frequency, as determined at sensor level at rest, was found in the alpha band for most participants. This individual peak frequency as well as the spectral power at that frequency at rest did not significantly change over the course of the experiment, nor did they correlate with the individual language performance.

Next, we turned to the MEG data acquired during task, by studying the spectral power attenuation at the individual peak frequency (as determined at rest). We tested our hypothesis that the individual power attenuation over the course of each sentence predicts the individual language comprehension performance. Indeed, we found correlations for, both, the power attenuation observed for the more complex sentences (double embedding) and the difference in power attenuation between the two complexity levels. While the same effects could be replicated when simply using the entire alpha band (8-12 Hz) instead of the individual peak frequency, the correlations were considerably weaker in that case. Interestingly, a spatial analysis based on a network atlas (Yeo's 17-networks) suggested that the difference between the power attenuations is present in a temporal-parietal network in the left hemisphere, while the effect of the double embedding condition alone localizes in its right hemisphere homologue.

Hence, in summary, the following observations underscore the functional role of these individually dominant (mostly alpha band) oscillations in language processing: (i) individual performance was correlated with alpha power attenuation during task but not with alpha power at rest, and (ii) these effects were localized in temporal-parietal brain regions usually associated with language processing.

Cortical alpha activity has been proposed to play an important role in excitability regulation mechanisms underlying various human cognitive abilities, including memory, attention, perception, etc. Task irrelevant regions exhibit higher alpha power reflecting inhibition, while in task relevant regions alpha power is reduced, reflecting increased excitability (Foxe & Snyder, 2011; Jensen & Mazaheri, 2010; Klimesch, 2012; Klimesch et al., 2007).

408   At rest, such an increased excitability could reflect a general predisposition of
409   a person towards cognitive performance. In contrast, if observed during task within
410   specific task relevant brain areas, it would index processes related to the particular
411   task or experimental situation. Alpha power at rest has been found to be positively
412   correlated with task performance in cognitive control (Mahjoory et al., 2019) and
413   episodic memory (Sargent et al., 2021) tasks, but negatively correlated with language
414   skills (Kwok et al., 2019). This somewhat non-univocal picture suggests that for
415   different experimental situations, different levels of pre-inhibition and disinhibition of
416   cortical areas are beneficial. On the other hand, during the actual task and within the
417   task relevant areas, we would expect a clear attenuation of alpha, which scales with
418   the actual engagement with the task reflected by task performance. There are a
419   number of previous studies showing general alpha attenuation during task within task
420   relevant areas (Hilla et al., 2020; Magosso et al., 2019; Wang et al., 2021). These
421   works show that the alpha oscillation power is related to the specific task demand.
422   This is reflected in our results by the finding that the individual alpha power
423   attenuation is stronger for the more complex sentences and increases with increasing
424   cognitive (including working memory) load along the sentence. On the other hand,
425   evidence for a correlation between alpha power modulation in specific task-relevant
426   brain areas and individual task performance is scarce. By clearly demonstrating this in
427   our study, we show that in-task alpha power attenuation actually reflects processes
428   that are involved in successful task completion.

429   Along with the idea that the association of the alpha power and performance
430   may indicate the task engagement of the brain regions, our results based on Yeo's 17-
431   networks suggest that the temporal-parietal network plays a crucial role in processing
432   the embedding. We further cross-checked and refined this by exploring the
433   association using the whole 360 ROI brain parcellation from the Glasser atlas and
434   found a particularly high association between power attenuation difference (double vs.
435   single) and performance in the superior temporal gyrus (Fig. S4. A). This is in
436   alignment with the literature showing that the posterior superior temporal gyrus plays
437   an important role in processing embedded structures (Friederici, 2011; Friederici et al.,
438   2006; Kinno et al., 2008; Röder et al., 2002). Regarding the differential findings in the
439   two homologue networks in the left and right hemispheres, we infer that even though
440   the areas in the left hemisphere form the classical language network (Friederici, 2011;
441   Hickok & Poeppel, 2004; Poeppel et al., 2012; Vigneau et al., 2006), homologue

442   areas in the right hemisphere may increasingly engage when task demands are high as
443   a result of enhanced working memory loads (Fridriksson & Morrow, 2005). This
444   would explain why we find right hemispheric effects for the double embedded
445   sentences, but not for the single embedded ones. Nevertheless, this notion alone
446   would predict effects for both embedding levels in the left hemisphere as well. Instead,
447   we only found an effect of the difference between these two levels, that is, on how
448   much the alpha power attenuation increases when the task complexity rises. How
449   could that be accounted for? One possible explanation is the following. Normal
450   language processing only engages the left hemisphere language areas and leads there
451   to an alpha power attenuation over the course of the sentence, which is strongly
452   individually specific. Some persons have a large attenuation and others a smaller one,
453   irrespective of the presented material. This causes a strong correlation between the
454   alpha power attenuation between single and double embedded sentences (Fig. 3D).
455   Then, there is an additional alpha power attenuation that is related to the cortical
456   engagement with the task, and hence to sentence complexity (Fig. 3C) and task
457   performance (Fig. 3E). While for each single condition (single and double embedding,
458   respectively) this correlation is obscured by the large inter-individual fluctuation, in
459   the difference between the two conditions this influence is cancelled out and the
460   correlation with performance becomes significant. The right hemisphere areas, in
461   contrast, are not so much involved in normal language processing and only step in to
462   cope with the high task demand in the double embedding condition. Therefore, the
463   alpha power attenuation is mainly task related and hence correlates with the task
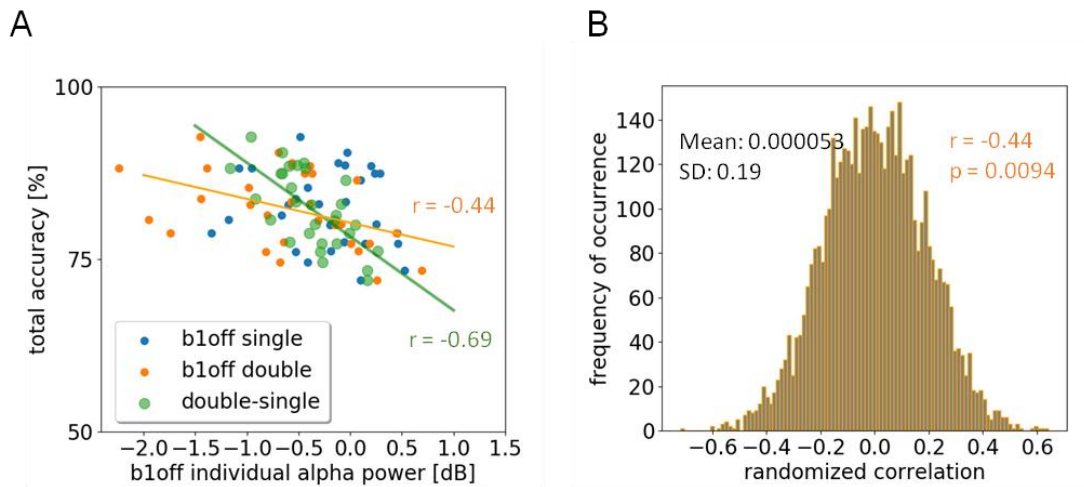464   performance.

465

5. Conclusion

467   In summary, in this present paper, we used a language comprehension
468   experiment to demonstrate that by manipulation of the task complexity, the alpha
469   power attenuation in the task relevant brain regions, especially the individual alpha,
470   reflect the increase of the cognitive load and predicted the individual performance
471   outcome. Individual alpha power could be a useful biomarker to highlight the relevant
472   brain regions and monitor the brain states during the cognitive processing.

473

474   ## 6. Supplementary Figures

475

476   Figure S1. Association between the individual peak frequency power attenuation at

477   the final closure of the embedded structure (*b1off*) and the total performance accuracy.

478   (A) Individual peak frequency power attenuation for double embedded sentences was

479   associated with the performance accuracy (Spearman's r = -0.44, p = 0.015). (B)

480   Permutation-test of the association between the individual peak frequency power

481   attenuation (*b1off*) for double embedded sentences and the performance accuracy. The

482   power attenuation values were permuted for 5000 times. The mean of the randomized

483   Spearman's correlation was 0.00 and the standard deviation was 0.19. The probability

484   of appearance of a correlation value less than r = -0.44 was 0.0094.

485

486

487
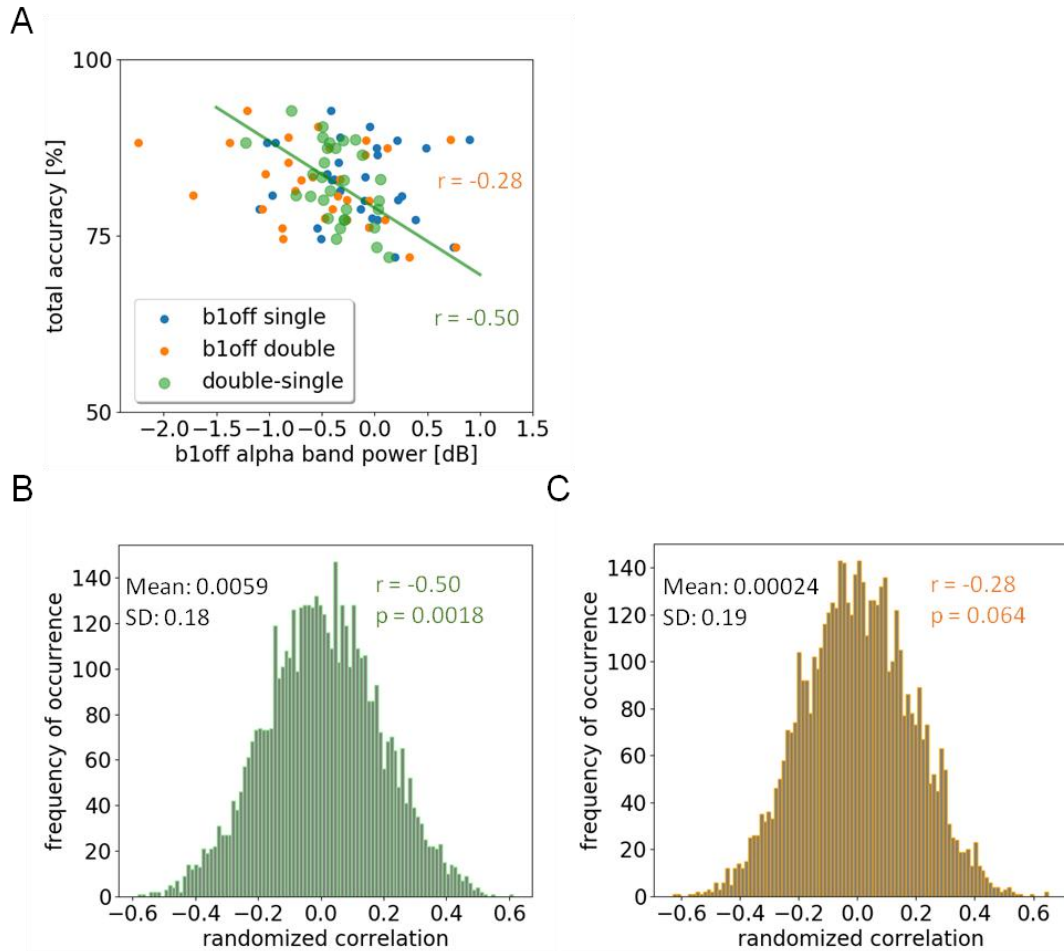
Figure S2. Association between the broad band alpha (8-12 Hz) power attenuation at the final closure of the embedded structure (*b1off*) and the total performance accuracy. (A) Broad band alpha power attenuation difference (double vs. single embeddings) associated with the total performance accuracy (Spearman's r = -0.50, p = 0.0049). (B) Permutation-test of the association between the broad band alpha power attenuation difference (double vs. single embedded sentence) at the final closure of the embeddings and the individual task performance. The power attenuations of the single as well as the double embedded sentences were permuted for 5000 times. The mean of the randomized Spearman's correlation was 0.0059 and the standard deviation was 0.18. The probability of appearance of a correlation value less than r = -0.50 was 0.0018. (C) Permutation-test of the association between the broad band alpha power attenuation (*b1off*) for double embedded sentences and the performance accuracy. The power attenuations were permuted for 5000 times. The mean of the randomized Spearman's correlation was 0.00024 and the standard deviation was 0.19. The probability of appearance of a correlation value less than r = -0.28 was 0.064.
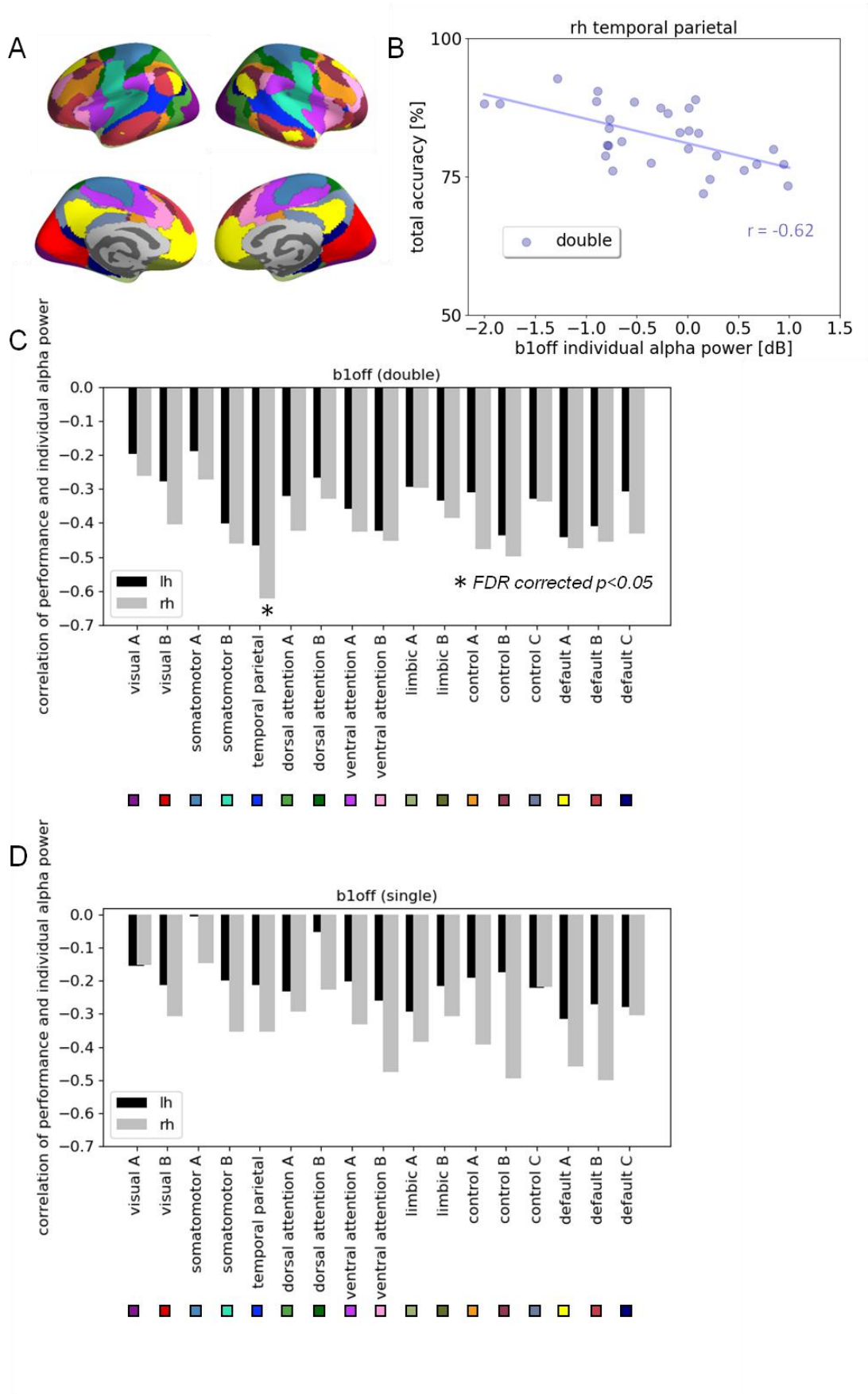
505

506

507

508

509

510

511   Figure S3. Association of the individual peak frequency power attenuation and the

512   language performance at the functional networks. (A) ROIs of Yeo's 17-networks.

513   Temporal parietal networks are marked with bright blue. (B) Individual peak

514   frequency power attenuation for double embedded sentences at the final closure of the

515   embedded structures (*b1off*) on the right temporal-parietal network was significantly

516   associated with the performance (Spearmans' r = -0.62, FDR corrected p<0.05)

517   (C)&(D) Spatial distribution of the Spearman's correlation between individual peak

518   frequency power attenuation of double (C) and single (D) embedded sentences at the

519   final closure of the embedded structures (*b1off*) and the individual performance

520   accuracy on Yeo's 17-networks.

521

522
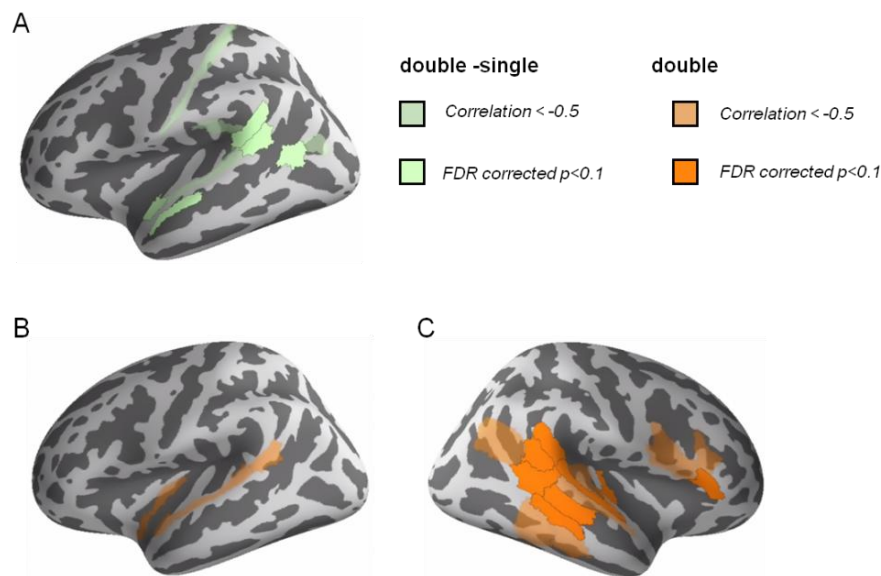
523
524

525   Figure S4. Association of the peak frequency power attenuation and the language

526   performance with the Glasser atlas. Spearman's correlation were calculated between

527   the total performance accuracy and the (i) power attenuation difference (double vs.

528   single embeddings) at the final closure of the embedded structure (b1off) as well as

529   the power attenuation at the final closure for (ii) double and (iii) single embedded

530   sentences for 360 ROIs. FDR-correction was based on all 1080 tests. Significant level

531   is p<0.1 (A) ROIs that showed the association between power attenuation difference

532   (douvle vs. Single embeddings) and the total performance accuracy. (B)&(C) ROIs

533   that showed the association between power attenuation for double embedded

534   sentences and the total performance accuracy.

535

536

A. Anke denkt nicht, dass Malte, der niemals ehrgeizig war, viele Muskeln hat.

b1on   b2on   b2off   b1off

Anke does not think that Malte, who was never ambitious, has many muscles.

Q: Hat Anke viele Muskeln? / *Does Anke have many muscles?*

B. Es war ihr klar, dass Henri, der Betty, die den Jungen adoptierte, fasziniert, glücklich ist.

b1on   b2on   b3on   b3off   b2off   b1off

It was clear to her that Henri, who fascinates Betty, who adopted the boy, is happy.

Q: Es war Betty, die Henri fasziniert, oder? / *It was Betty who fascinated Henri, wasn't it?*

537

538

539

540 Figure S5. Examples of presented sentences in German with English translations in
541 italics: (A) single; (B) double center embedding. We used the data segment starting at
542 *b1on* as a reference to compute the relative alpha power attenuation for all other
543 marked time points. The marker *b1on* represented the beginning of the relative clause
544 containing all hierarchical embedding. Q: Probing questions for the presented
545 examples.

546
547
548
549
550
551
552
553
554
555
556
557
558
559
560
561
562
563

7. References

Berger, H. (1938). Über das Elektrenkephalogramm des Menschen. XIV. *Archiv Für Psychiatrie Und Nervenkrankheiten*.

Foxe, J. J., & Snyder, A. C. (2011). The role of alpha-band brain oscillations as a sensory suppression mechanism during selective attention. *Frontiers in Psychology*, *2*(JUL), 1–13. https://doi.org/10.3389/fpsyg.2011.00154

Fridriksson, J., & Morrow, L. (2005). Cortical activation and language task difficulty in aphasia. *Aphasiology*, *19*(3–5), 239–250.

Friederici, A. D. (2011). The brain basis of language processing: from structure to function. *Physiological Reviews*, *91*(4), 1357–1392.

Friederici, A. D., Bahlmann, J., Heim, S., Schubotz, R. I., & Anwander, A. (2006). The brain differentiates human and non-human grammars: Functional localization and structural connectivity. *Proceedings of the National Academy of Sciences of the United States of America*, *103*(7), 2458–2463. https://doi.org/10.1073/pnas.0509389103

Furman, A. J., Meeker, T. J., Rietschel, J. C., Yoo, S., Muthulingam, J., Prokhorenko, M., Keaser, M. L., Goodman, R. N., Mazaheri, A., & Seminowicz, D. A. (2018). Cerebral peak alpha frequency predicts individual differences in pain sensitivity. *NeuroImage*, *167*, 203–210.

Gastaldon, S., Arcara, G., Navarrete, E., & Peressotti, F. (2020). Commonalities in alpha and beta neural desynchronizations during prediction in language comprehension and production. *Cortex*, *133*, 328–345. https://doi.org/10.1016/j.cortex.2020.09.026

Glasser, M. F., Coalson, T. S., Robinson, E. C., Hacker, C. D., Harwell, J., Yacoub, E., Ugurbil, K., Andersson, J., Beckmann, C. F., & Jenkinson, M. (2016). A multi-modal parcellation of human cerebral cortex. *Nature*, *536*(7615), 171–178.

Grabot, L., & Kayser, C. (2020). Alpha activity reflects the magnitude of an individual bias in human perception. *Journal of Neuroscience*, *40*(17), 3443–3454.

Gramfort, A., Luessi, M., Larson, E., Engemann, D. A., Strohmeier, D., Brodbeck, C., Goj, R., Jas, M., Brooks, T., & Parkkonen, L. (2013). MEG and EEG data analysis with MNE-Python. *Frontiers in Neuroscience*, *7*, 267.

Gulbinaite, R., van Viegen, T., Wieling, M., Cohen, M. X., & VanRullen, R. (2017). Individual alpha peak frequency predicts 10 Hz flicker effects on selective attention. *Journal of Neuroscience*, *37*(42), 10173–10184.

Hickok, G., & Poeppel, D. (2004). Dorsal and ventral streams: a framework for understanding aspects of the functional anatomy of language. *Cognition*, *92*(1–2), 67–99.

Hilla, Y., von Mankowski, J., Föcker, J., & Sauseng, P. (2020). Faster Visual Information Processing in Video Gamers Is Associated With EEG Alpha Amplitude Modulation. *Frontiers in Psychology*, *11*, 3333.

601   Horschig, J. M., Jensen, O., van Schouwenburg, M. R., Cools, R., & Bonnefond, M. (2014). Alpha
602   activity reflects individual abilities to adapt to the environment. *NeuroImage*, *89*, 235–243.
603   Jensen, O., & Mazaheri, A. (2010). Shaping functional architecture by oscillatory alpha activity: gating
604   by inhibition. *Frontiers in Human Neuroscience*, *4*, 186.
605   Jones, S. R., Kerr, C. E., Wan, Q., Pritchett, D. L., Hämäläinen, M., & Moore, C. I. (2010). Cued spatial
606   attention drives functionally relevant modulation of the mu rhythm in primary somatosensory
607   cortex. *Journal of Neuroscience*, *30*(41), 13760–13765.
608   Katyal, S., He, S., He, B., & Engel, S. A. (2019). Frequency of alpha oscillation predicts individual
609   differences in perceptual stability during binocular rivalry. *Human Brain Mapping*, *40*(8), 2422–
610   2433.
611   Kinno, R., Kawamura, M., Shioda, S., & Sakai, K. L. (2008). Neural correlates of noncanonical syntactic
612   processing revealed by a picture-sentence matching task. *Human Brain Mapping*, *29*(9), 1015–
613   1027.
614   Klimesch, W. (2012). Alpha-band oscillations, attention, and controlled access to stored information.
615   *Trends in Cognitive Sciences*, *16*(12), 606–617. https://doi.org/10.1016/j.tics.2012.10.007
616   Klimesch, W., Pfurtscheller, G., Mohl, W., & Schimke, H. (1990). Event-related desynchronization,
617   ERD-mapping and hemispheric differences for words and numbers. *International Journal of*
618   *Psychophysiology*, *8*(3), 297–308.
619   Klimesch, W., Sauseng, P., & Hanslmayr, S. (2007). EEG alpha oscillations: the inhibition–timing
620   hypothesis. *Brain Research Reviews*, *53*(1), 63–88.
621   Kwok, E. Y. L., Cardy, J. O., Allman, B. L., Allen, P., & Herrmann, B. (2019). Dynamics of spontaneous
622   alpha activity correlate with language ability in young children. *Behavioural Brain Research*, *359*,
623   56–65. https://doi.org/10.1016/j.bbr.2018.10.024
624   Magosso, E., De Crescenzio, F., Ricci, G., Piastra, S., & Ursino, M. (2019). EEG alpha power is
625   modulated by attentional changes during cognitive tasks and virtual reality immersion.
626   *Computational Intelligence and Neuroscience*, *2019*. https://doi.org/10.1155/2019/7051079
627   Mahjoory, K., Cesnaite, E., Hohlefeld, F. U., Villringer, A., & Nikulin, V. V. (2019). Power and temporal
628   dynamics of alpha oscillations at rest differentiate cognitive performance involving sustained
629   and phasic cognitive control. *Neuroimage*, *188*, 135–144.
630   Mann, C. A., Sterman, M. B., & Kaiser, D. A. (1996). Suppression of EEG rhythmic frequencies during
631   somato-motor and visuo-motor behavior. *International Journal of Psychophysiology*, *23*(1–2), 1–
632   7.
633   Migliorati, D., Zappasodi, F., Perrucci, M. G., Donno, B., Northoff, G., Romei, V., & Costantini, M.
634   (2020). Individual alpha frequency predicts perceived visuotactile simultaneity. *Journal of*
635   *Cognitive Neuroscience*, *32*(1), 1–11.
636   Minami, S., Oishi, H., Takemura, H., & Amano, K. (2020). Inter-individual differences in occipital alpha
637   oscillations correlate with white matter tissue properties of the optic radiation. *Eneuro*, *7*(2).
638   Pfurtscheller, G. (1989). Functional Topography During Sensorimotor Activation Studied with Event-

639   Related Desynchronization Mapping. *Journal of Clinical Neurophysiology*, *6*(1), 75–84.

640   https://doi.org/10.1097/00004691-198901000-00003

641 Pfurtscheller, G. (2003). Induced Oscillations in the Alpha Band: Functional Meaning. *Epilepsia*, *44*(12

642   SUPPL.), 2–8. https://doi.org/10.1111/j.0013-9580.2003.12001.x

643 Poeppel, D., Emmorey, K., Hickok, G., & Pylkkänen, L. (2012). Towards a new neurobiology of

644   language. *Journal of Neuroscience*, *32*(41), 14125–14131.

645 Rathee, S., Bhatia, D., Punia, V., & Singh, R. (2020). Peak Alpha Frequency in Relation to Cognitive

646   Performance. *Journal of Neurosciences in Rural Practice*, *11*(3), 416–419.

647   https://doi.org/10.1055/s-0040-1712585

648 Röder, B., Stock, O., Neville, H., Bien, S., & Rösler, F. (2002). Brain activation modulated by the

649   comprehension of normal and pseudo-word sentences of different processing demands: a

650   functional magnetic resonance imaging study. *Neuroimage*, *15*(4), 1003–1014.

651 Sadaghiani, S., & Kleinschmidt, A. (2016). Brain networks and α-oscillations: structural and functional

652   foundations of cognitive control. *Trends in Cognitive Sciences*, *20*(11), 805–817.

653 Sargent, K., Chavez-Baldini, U., Master, S. L., Verweij, K. J. H., Lok, A., Sutterland, A. L., Vulink, N. C.,

654   Denys, D., Smit, D. J. A., & Nieman, D. H. (2021). Resting-state brain oscillations predict cognitive

655   function in psychiatric disorders: A transdiagnostic machine learning approach. *NeuroImage:*

656   *Clinical*, *30*, 102617.

657 Schomer, D. L., & Da Silva, F. L. (2012). *Niedermeyer's electroencephalography: basic principles,*

658   *clinical applications, and related fields*. Lippincott Williams & Wilkins.

659 Sklar, B., Hanley, J., & Simmons, W. W. (1972). An EEG experiment aimed toward identifying dyslexic

660   children. *Nature*, *240*(5381), 414–416.

661 Smit, C. M., Wright, M. J., Hansell, N. K., Geffen, G. M., & Martin, N. G. (2006). Genetic variation of

662   individual alpha frequency (IAF) and alpha power in a large adolescent twin sample.

663   *International Journal of Psychophysiology*, *61*(2), 235–243.

664 Thomas Yeo, B. T., Krienen, F. M., Sepulcre, J., Sabuncu, M. R., Lashkari, D., Hollinshead, M., Roffman,

665   J. L., Smoller, J. W., Zöllei, L., & Polimeni, J. R. (2011). The organization of the human cerebral

666   cortex estimated by intrinsic functional connectivity. *Journal of Neurophysiology*, *106*(3), 1125–

667   1165.

668 Van Dijk, H., Schoffelen, J.-M., Oostenveld, R., & Jensen, O. (2008). Prestimulus oscillatory activity in

669   the alpha band predicts visual discrimination ability. *Journal of Neuroscience*, *28*(8), 1816–1823.

670 van Ede, F., Köster, M., & Maris, E. (2012). Beyond establishing involvement: quantifying the

671   contribution of anticipatory α-and β-band suppression to perceptual improvement with

672   attention. *Journal of Neurophysiology*, *108*(9), 2352–2362.

673 Van Veen, B. D., Van Drongelen, W., Yuchtman, M., & Suzuki, A. (1997). Localization of brain electrical

674   activity via linearly constrained minimum variance spatial filtering. *IEEE Transactions on*

675   *Biomedical Engineering*, *44*(9), 867–880.

676 Vigneau, M., Beaucousin, V., Hervé, P.-Y., Duffau, H., Crivello, F., Houde, O., Mazoyer, B., & Tzourio-

677   Mazoyer, N. (2006). Meta-analyzing left hemisphere language areas: phonology, semantics, and

678   sentence processing. *Neuroimage*, *30*(4), 1414–1432.

679 Wang, P., Knösche, T. R., Friederici, A. D., Maess, B., Chen, L., & Brauer, J. (2021). Functional brain

680   plasticity during L1 training on complex sentences : Changes in gamma-band oscillatory activity.

681   *Human Brain Mapping*, *March*, 1–13. https://doi.org/10.1002/hbm.25470

682 Wobbrock, J. O., Findlater, L., Gergle, D., & Higgins, J. J. (2011). The aligned rank transform for

683   nonparametric factorial analyses using only anova procedures. *Proceedings of the SIGCHI*

684   *Conference on Human Factors in Computing Systems*, 143–146.

685